Photo-induced Energy Transfer Polymerization

Jian Liu[1], Yaxiong Wei[2], Liangwei Ma[1], Xin Jin[1], Siyu Sun[1], Meng Liu[3], Jun Du[3, 4], Xinsheng Xu[2], He Tian[1], Xiang Ma[1]*

[1]Key Laboratory for Advanced Materials and Feringa Nobel Prize Scientist Joint Research Center, Frontiers Science Center for Materiobiology and Dynamic Chemistry, School of Chemistry and Molecular Engineering, East China University of Science and Technology, Meilong Road 130, Shanghai 200237 (P. R. China).

[2]Anhui Province Key Laboratory of Optoelectric Materials Science and Technology, School of Physics and Electronic Information, Anhui Normal University, Wuhu 241002, China.

[3]State Key Laboratory of Molecular Reaction Dynamics, Dalian Institute of Chemical Physics, Chinese Academy of Sciences, Dalian, Liaoning 116023, China.

[4]University of Chinese Academy of Sciences, Beijing 100049, China.

*Corresponding author. Email: maxiang@ecust.edu.cn

Abstract: In conventional photo-induced polymerization strategies, the active species that initiate the reaction tend to be exogenous radical species. Inspired by photo-induced cycloaddition reactions, in this study we investigated photo-induced polymerization from the perspective of energy transfer processes. Utilizing low-energy, highly reactive triplet species of olefin molecules as energy acceptors, a polymerization strategy without the need for exogenous active components was developed. Triplet species from various sources were able to induce polymerization, demonstrating the excellent versatility of this strategy. The reaction mechanism was thoroughly investigated with controlled experiments and spectroscopic methods using thiochromanone as a template. It was clearly established that the key to polymerization is an active triplet species rather than a conventional radical species. As a result, the findings of this study stimulate further discussion on the role of monomers in photo-induced polymerization.

One-Sentence Summary: A novel, facile, and universal photo-induced polymerization method was derived based on a triplet-triplet energy transfer (TTET) process.

Photo-induced energy transfer processes have been widely applied to the design of optical devices, solar cells, and photocatalysts (*1, 2*). For example, cycloaddition (*3, 4*), bond dissociation (*5, 6*), and transition metal sensitization (*7, 8*) in coupling reactions have been carried out by the photo-induced energy transfer process. In these processes, a catalyst becomes photoexcited and undergoes triplet–triplet energy transfer with the reactants, which in turn excites them to the active triplet state by crossing the energy gap. Among these reactions, the excitation wavelengths of many photocatalysts have been extended to the visible region (*2*).

Acrylate molecules are very difficult to directly excite, and therefore their photo-induced polymerization reactions are often mediated by exogenous radical species. Controlled living radical polymerization (CLRP), an efficient method for the synthesis of polymers with more complex and well-defined structures, uses light as an initiator and regulatory switch for the reaction (*9-11*). A series of organic photocatalysts (PC) based on phenazine and phenothiazine were developed by Hawker and Miyake to achieve photo-controlled atom transfer radical polymerization (ATRP) (*12-15*). Oxygen-doped anthanthrene has also been noted for its lower catalytic loadings (*16, 17*). Kwon et al. designed an array of organic photocatalysts with computational assistance to elucidate the conformational relationships in an O-ATRP process (*18*). Photo energy transfer reversible addition-fragmentation chain transfer (PET-RAFT) polymerization was achieved through RAFT reagent engineering by Boyer et al. (*19-21*). An abundance of photopolymerization methods can expand the range of applicable monomers (*22-26*) and optimize reaction conditions (*27-29*). However, all these methods rely on the addition of exogenous radical species to achieve photopolymerization. Some cases involve more than three components including monomer, photocatalyst, initiator, and modifier, thus complicating the system (*30, 31*). In addition, most discussions of photo-CLRP tend to focus on the photochemical processes of catalysts, initiators, and modifiers, ignoring the role that the acrylate itself plays in the reaction. By revisiting photo-induced polymerization using the perspective of energy transfer processes, the potential of acrylates to act as energy acceptors is revealed. This promotes our knowledge of polymerization reactions and assists in the design of polymerization methods with simpler components and more general applicability.
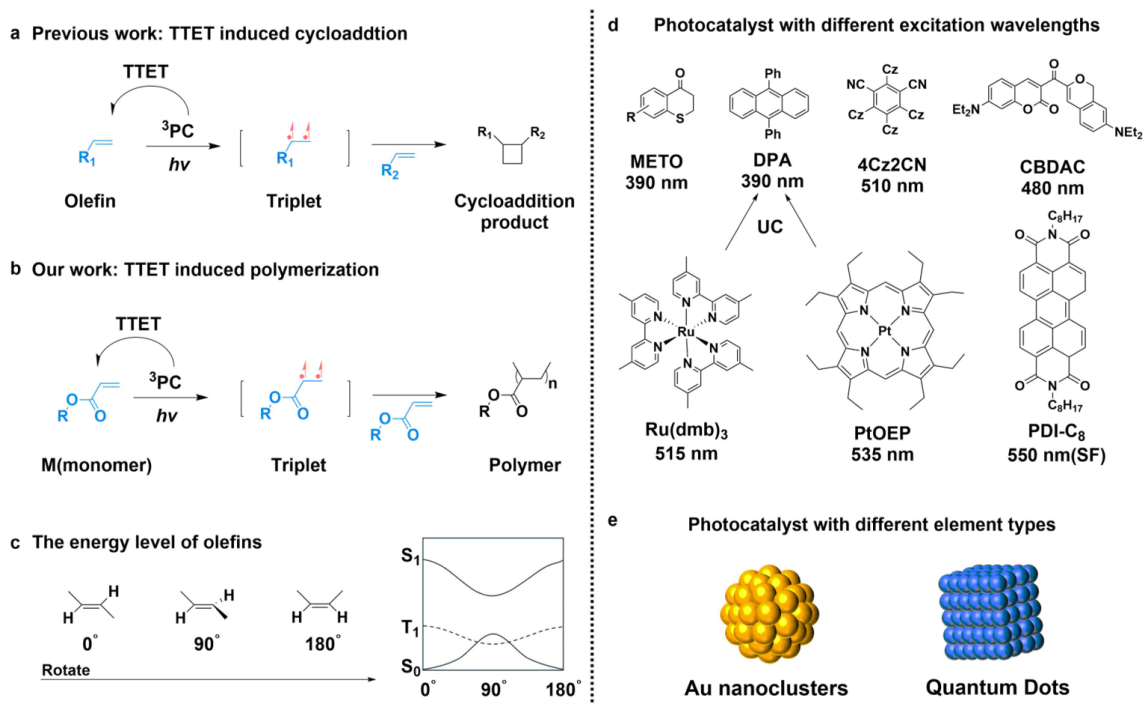
Figure 1. The process of photo-induced energy transfer polymerization. Proposed mechanism of (**a**) TTET-induced cycloaddition reaction and (**b**) TTET-induced polymerization. (**c**) The energy level of olefins. (**d**) and (**e**) Various photocatalysts mentioned in this article. PC: photocatalyst, UC: upconversion, SF: singlet fission, TTET: triplet-triplet energy transfer, Cz: carbazole.

Herein, inspired by the mechanism of partial cycloaddition reactions (Figure 1a) (*4, 32*), it was realized that triplets of olefin molecules act as an active species in addition reactions. Moreover, acrylates are a special class of olefins that are often used as monomers in polymerization reactions. These facts aroused our interest in the polymerization of acrylates using triplet-state processes. This would differ from conventional radical polymerization, which is initiated by radicals generated by photocleavage of organic molecules, and would be significantly distinguished from photo-CLRP, which controls the behavior of the active species through a photo-induced reversible reaction.

Acrylates commonly have very weak conjugated structures, which result in a high S_1 energy level (>4.0 eV) and almost no absorption in the UV–visible region (Figure S12

). However, their double bonds rotate in the triplet state (Figure 1c), and this rotation causes energy dissipation, resulting in their T_1 potential energy surface crossing with the S_0 potential energy surface. This mechanism has been used to design photo-induced double-bond isomerization (*33, 34*). As a result, the T_1 energy level of acrylates (about 2.6 eV) is much lower than the S_1 energy level, which is difficult to reach through intersystem crossing (ISC) (Figure 1c). The lower T_1 energy level also implies that acrylates are TTET acceptors for many photosensitizers. Therefore, photo-polymerization may take place in more simplistic systems and allow the wavelength of the light source for photopolymerization to shift to as long a region as possible. The lifetimes of singlet states are generally less than one-thousandth of the triplet states (*35*), and thus the contribution of the singlet states in the energy transfer process is negligible. With this recognition, it is only the occurrence of the TTET process that is discussed in this paper.

Results and discussion

3

Based on the recognition of the TTET process, a two-component catalytic polymerization reaction merely consisting of the photocatalyst and the monomer was deemed attainable. During this process, the acrylate works as an acceptor that is excited to the triplet state by an energy transfer process and becomes the initiation point of the chain reaction (Figure 1b). Methoxyl-substituted thiochroman-4-one (METO), CBDAC, and 4Cz2CN (Figure 1d) were selected as TTET donors, and their absorption wavelength distributions continuously covered the spectral range from 390 to 510 nm (Figure S8).

Table 1. Polymerization using various photocatalysts. Conversions were determined by NMR. Methyl methacrylate (MMA) as the monomer, reaction time = 24 h, PC loading = 500 ppm (relative to monomer), RT. (**a**) PEGMA$_{480}$ as the monomer. (**b**) Conversions were determined by weight. PtOEP: platinum octaethylporphyrin. Ru(dmb)$_3$: Tris(4,4'-dimethyl-2,2'-bipyridine) ruthenium(II).

	PC	Light (nm)	E_{T1} (eV)	Solvent	Conv (%)
1	METO-1	390	2.66	THF	92.2
2	CBDAC	480	2.38	THF	90.9
3	4Cz2CN	510	2.51	THF	81.3
4	AuNCs	365	/	H_2O_a	42.5[b]
5	CsPbBr$_3$-OA	365	/	Hex	48.3[b]
6	CsPbBr$_3$-RhB	365	/	Hex	51.2[b]
7	DPA	390	>2.88(TTA)	DCM	55.6
8	Ru(dmb)$_3$-DPA	510	>2.88(TTA)	MeCN	32.4
9	Ru(dmb)$_3$	510	2.02	MeCN	0
10	PtOEP-DPA	530	>2.88(TTA)	DCM	27.0
11	PtOEP	530	1.90	DCM	0
12	CdSe-TCA-DPA	530	>2.88(TTA)	Hex	26.4[b]
13	CdSe	530	/	Hex	0
14	PDI-C$_8$	550	2.96(SF)	Tol	68.2

The selected molecules with different excitation wavelengths all succeeded in catalyzing the photo-induced polymerization of MMA (Table 1). The photo-induced polymerization by all the molecules was completed within 24 h, and high final conversions of 92.2% and 90.9% were achieved by METO-1 and 4Cz2CN, respectively. Triplet donor molecules with different structures and photochemical properties exhibited similar catalytic activity, undoubtedly demonstrating the universality and generality of the reaction.

Under continuous light excitation, organic molecules may cleave and generate radicals that initiate polymerization reactions of monomers. Certain conventional radical initiators were designed based on this cleavage, such as azobisisobutyronitrile and dibenzoyl peroxide. As early as the 1980s, electron paramagnetic resonance (EPR) spectra were used to observe free radical processes in the polymerization of acrylates (*36-39*). Time-resolved electron paramagnetic resonance (TR-EPR) was able to observe the generation and decay of these radicals (*40*). In an effort to appreciate the completely innovative polymerization mechanism in this study, TR-EPR was used to capture radical species to exclude the effect of this process on the energy transfer-induced polymerization reaction. TR-EPR experiments were undertaken for the METO-1 and METO-3 reaction systems before and after the addition of MMA, and no EPR peaks were detected (Figures S32 and S33) in the wider spectral range (330–340 mT). This indicated that no observable radicals were generated either by METO as a catalyst or by the monomer during the reaction. Therefore,

4

this experiment excluded the influence of radicals generated by photocleavage of organic molecules on the reaction process in the system.

These energy transfer processes do not occur only between organic molecules and monomers. Some quantum dots (QDs) and Au nanoclusters (Au NCs) are favorable candidates for study, as they possess similar photochemical properties as those of organic molecules. The recently reported $CsPbBr_3$ QDs with surface-anchored Rhodamine B enabled the efficient generation of triplet states by charge separation and the spin-flip mechanism (*41*). This QD was also successfully applied to photo-induced polymerization, in which it demonstrated a tight correlation between the polymerization process and the energy transfer process. To verify the findings, olein acid (OA)-modified $CsPbBr_3$ QDs were also selected as a photocatalyst for the polymerization, and similar results were obtained. Another inorganic catalyst, an Au@α-CD NC (Au NC) system stabilized in an aqueous phase, derives its properties from its nano-size effect. $PEGMA_{480}$ was used as a monomer in a photo-induced polymerization in an aqueous phase catalyzed by Au NCs, and the polymerization was also successful under similar yet different conditions. This suggests that energy transfer-induced polymerization is broadly universal and does not depend on the catalyst type or solvent environment. The successful results convinced us of the existence of energy transfer and aroused our interest in its further study. The photochemical properties of these systems derive from a core consisting of inorganic elements, particularly OA-modified $CsPbBr_3$ QDs and Au NCs, which are free of organic ligands with UV–visible absorption. Using these photocatalysts excludes the possibility of generating free radicals from the cleavage of organic molecules under continuous irradiation. Their low conversion was due to the large proportion of acylates in the reaction system (1:2 relative to the solvent, by volume), which increased the polarity of the solvent and caused some agglomeration of the quantum dots.

The only requirement for selecting a photocatalyst is an appropriate triplet state energy level. With the energy condition satisfied, the polymerization can be induced by any triplets generated by various photophysical processes. Diphenylanthracene (DPA) is a common upconversion annihilator with fluorescence emission at about 430 nm. A transition triplet species with a higher energy level than that of the singlet state arises during the triplet‒triplet annihilation process (*42-44*), which generated a 55.6% polymerization conversion under direct excitation. $Ru(dmb)_3$ and PtOEP acting as photosensitizers transferred their energy to DPA through an upconversion process under excitation of 510 and 530 nm light. The energy levels of their own triplet states are too low to induce polymerization, but with the addition of DPA as an annihilating agent, polymerization occurred. Due to the limited efficiency of the upconversion process, the conversion rates of polymerization for these two approaches were only 32.4% and 27.0%. The triplet state of $PDI-C_8$ has an energy level of about 1.48 eV, which is not sufficient for TTET with monomer molecules, whereas a triplet state with double energy (2.96 eV) can be generated by singlet fission (*45*), which in turn induces a polymerization reaction.
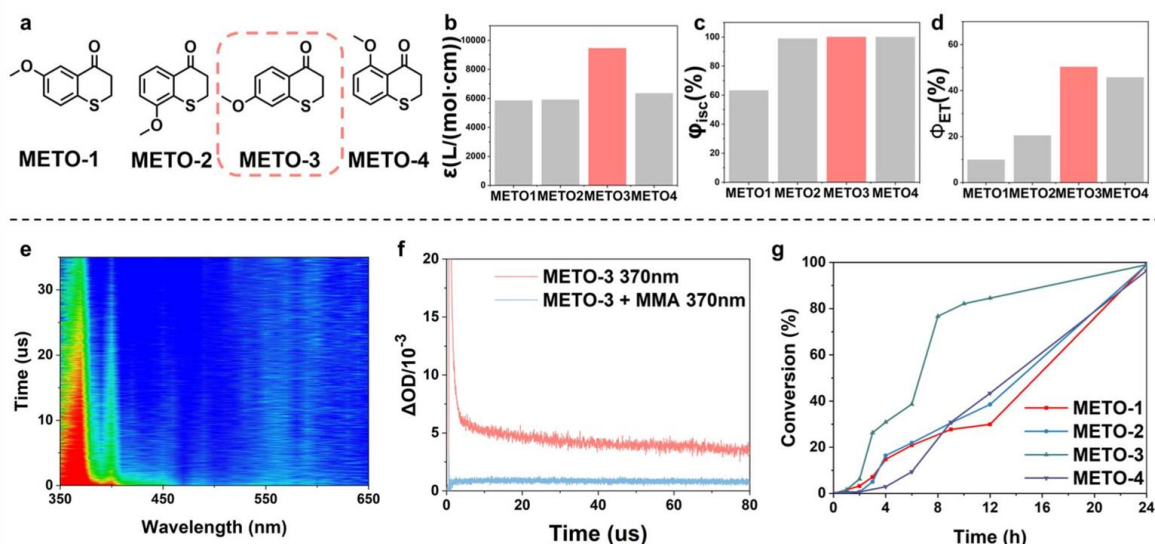
Figure 2. The spectrum data and catalytic performance of METO. (**a**) The structure of METO-1–4. (**b**) The molar absorption coefficient of METO-1–4. (**c**) The ISC efficiency of METO-1–4. (**d**) The TTET efficiency between METO-1–4 and MMA. (**e**) The transition absorption (TA) spectra of METO-3. (**f**) The kinetic curve @370 nm of METO-3 before and after the addition of MMA. (**g**) The kinetic curve of the polymerization catalyzed by METO-1–4.

To guide the design and selection of photocatalysts for energy transfer polymerization, the feasibility and mechanism of this energy transfer phenomenon first needed to be investigated. According to the reaction mechanism proposed in Figure 1b, the accumulation of triplet species is critical for initiating the polymerization reaction. Based on this presumption, the molar absorption coefficient, ISC efficiency, and TTET efficiency are all considered important factors contributing to the generation and accumulation of triplet species.

Methoxyl-substituted thiochroman-4-one (METO) derivatives (Figure 2a) are a class of molecules with unusual phosphorescent properties, which were carefully studied by Ma et al. (*46, 47*). METO-1 to METO-4 molecules are isomers with different methoxy substituent positions, in which the molecular backbones are identical to single benzene structures. In addition to the varied position of the methoxy substituent, METO-1–4 can undergo significant changes in their molecular orbital distributions, which in turn change their k_f and thus greatly enhance their ISC efficiency for switching from fluorescence emission to phosphorescence.

To further elucidate the photochemical processes between METO molecules and MMA, we performed transient absorption experiments on the nanosecond scale (Figures S17–S29). As a class of molecules with millisecond lifetimes of phosphorescence emission at 77 K, the triplet species of METO are clearly and readily observed on transient absorption spectra. Consequently, such systems are suited for revealing their photochemical processes by comparing the positions of transient absorption peaks and kinetic decay curves in the presence and absence of MMA. For METO-3, the full-spectrum transient absorption quench after the addition of MMA was so pronounced that all transient absorption peaks within 300–800 nm were almost completely invisible (Figure 2e). The kinetic curve of METO-3 showed a long-lived species of 50.7 μs at 370 nm and shorter lifetime species at 480 (0.42 μs) and 530 nm (0.64 μs). After the addition of MMA, there was no signal that could be fitted at 370 nm (Figure 2f) or two other wavelengths. The quenching of the transient absorption spectra further confirmed the existence of the TTET process.

6

Combined with a comparison of the molar extinction coefficients, the ISC efficiencies, and the ET efficiencies (estimated by the quenching of the phosphorescent lifetimes), METO derivatives were predicted to be an efficient catalyst. METO-3 was considered to have the best catalytic performance (Figure 2b–d), and the catalytic performances of METO-3 and METO-4 were better than those of METO-1 and METO-2. The kinetic curves of the photo-induced polymerizations were consistent with our expectations, with all four METOs achieving more than 90% catalytic conversion, while METO-3 had the highest conversion rate (Figure 2g). Unfortunately, there were no transient absorbing species found for the energy transfer product, probably due to the lower rate of generation and accumulation of the triplet species of MMA, making it difficult to accumulate detectable concentrations over the time scales tested.

Table 2. Catalytic performance of METO-1–4. MMA as the monomer, reaction time = 24 h, light source = 390 nm, RT.

PC	Loading (ppm)	Solvent	Conv (%)
METO1	100	THF	65.3
METO1	500	THF	92.2
METO2	100	THF	85.5
METO2	500	THF	>99
METO3	100	THF	95.6
METO3	500	THF	>99
METO4	100	THF	96.0
METO4	500	THF	>99

Delicate experimental catalytic polymerization tests were carried out to visualize the effect of METO with different substituent positions on catalytic polymerization. The reaction proceeded readily at 100 ppm (relative to the monomer), and 500 ppm was sufficient for an almost complete conversion of MMA (Table 2). The photocatalytic performance of METO-1–4 was also consistent with the predictions. METO-1 had the lowest molar extinction coefficient, ISC rate, and energy transfer efficiency, and thus the lowest yield of the polymerization reaction. However, the molecular weight distributions were in the range of 1.3–1.5 under certain conditions, which was attributed to a lower reaction rate that eliminated several chain transfer and termination reactions. The catalytic performance of METO-3 and METO-4 was then regulated with a RAFT agent, which achieved narrow molecular weight distributions (1.1) and high initiation efficiencies (>90%) under suitable conditions (Table S9).
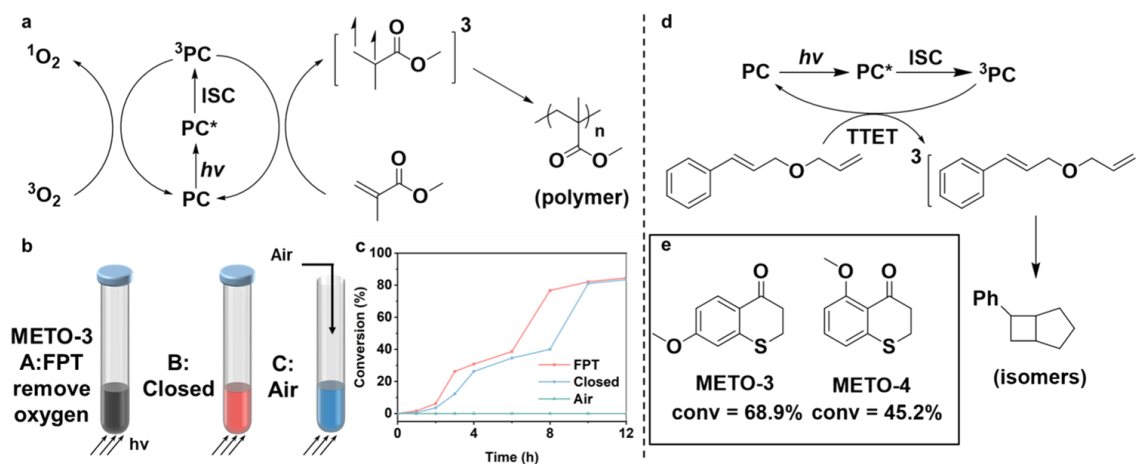
Figure 3. Experiments verifying the mechanism. (**a**) Scheme of TTET-induced photopolymerization. (**b**) Illustration of three different reaction conditions. (**c**) Polymerization rate profiles of METO-3 in three different oxygen environments. (**d**) A classical triplet-sensitized cycloaddition reaction. (**e**) Conversion of METO-3 to METO-4 as a photocatalyst for the reaction in (**d**). Reaction time = 6 h.

Aiming to demonstrate the causality between the energy transfer process and the polymerization process, a comparative experiment of triplet-state quenching was introduced to provide evidence by observing the rates and conversions of the reaction. Oxygen is a specific molecule with a triplet state ($^3O_2$) as its ground state, enabling TTET with photosensitizers, and thus it is also a sensitive triplet-state quenching agent. The product of the TTET process is highly oxidizing singlet oxygen ($^1O_2^*$, Figure 3a), in which the excitation energy is as low as 0.98 eV (1265 nm) (*48*), which could not induce polymerization. A radical process may also be inhibited by oxygen, yet we already excluded the effect of the radical process by TR-EPR in the previous discussion (Figures S32 and S33).

Therefore, a control experiment was designed in which each reaction was carried out in parallel in three groups under different conditions. The deoxygenation conditions in the first group were controlled as three freeze thaw cycles of deoxygenation and nitrogen filling. In the second group, the reaction system was closed to limit the oxygen content. In the third group, air was continuously passed in small volumes through an air pump to ensure fresh dissolved oxygen in the solution at all times (Figure 3b). From the kinetic curves, it was evident that the rate of the second group using the closed system showed significant curve retardation in comparison with the rate curve of the first group, which indicated that there was a significant kinetic induction period in the reaction (Figure 3c). In the first group, the freeze thaw cycle produced deoxygenation, with almost no evidence of the TTET process between METO-3 and $^3O_2$, and the production and accumulation of active species started immediately. In the second group, the quenching process of oxygen proceeded first, and the accumulation of triplet reactive species began afterward. By 10–12 h, the conversions gradually tended to converge, which also indicated that the catalytic process is not a conventional radical-initiated process, and the catalyst is quenched rather than consumed by the oxygen. There was only minimal polymerization because the pathways for the production and accumulation of active species were continuously inhibited by the continuous drumming of air in the third group. The same experiments were performed using METO-4, and an induction period was also observed (Figure S30).

METO catalysts were also used for the photocatalysis of another well-studied and reliable triplet-sensitized photochemical reaction(*3*) to verify the rationality of the mechanism (Figure 3d). Cycloaddition reactions using METO-3 and METO-4 as catalysts were both successful, suggesting that there is an intrinsic correlation between the mechanisms of the two reactions. The fact that the reaction proceeded in two distinct pathways was due to differences in the structure and concentration of the reactants.
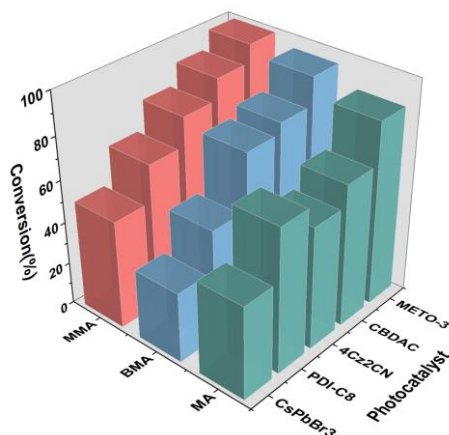
Figure 4. Catalytic performance of various photocatalysts with other acrylate monomers. PC loading = 500 ppm (relative to monomer), reaction time = 24 h, RT.

For ensuring the broad scope of this strategy, experiments of the catalytic polymerization of butyl Methacrylate (BMA) and methyl acrylate (MA) by several other selected photocatalysts were also conducted (Figure 4, details in Tables S6–S8). Within a larger range of monomers, the photocatalytic polymerization reaction remained capable of proceeding, and the distribution of the yields achieved followed a similar trend to that exhibited by MMA.

Conclusion

In conclusion, a novel photo-induced polymerization reaction pathway has been developed. The TTET process was successfully applied to excite monomer molecules to the triplet state as a starting point for chain reactions. According to the properties of the polymerization, the option of photocatalysts is wide, including common organic molecules, as well as inorganic systems with similar photochemical properties. Photo-induced energy transfer polymerization has less stringent requirements on the ISC efficiency of the photocatalyst, and the small amount of triplet species generated by upconversion and singlet fission can meet the demand. The excellent universality of the TTET process simplifies the components of the polymerization system and certainly broadens the application potential of polymerization. The mechanism of the reaction was investigated and insightfully summarized using transient spectroscopy, and TR-EPR was used to exclude interference from conventional radical polymerization. Based on the postulated reaction mechanism, photocatalysts were designed and selected, and the expected properties obtained. The results of TR-EPR confirm the existence of this process as distinguished from conventional radical polymerization.

References

1. S. Dutta, J. E. Erchinger, F. Strieth-Kalthoff, R. Kleinmans, F. Glorius, Energy transfer photocatalysis: exciting modes of reactivity. *Chem. Soc. Rev.* **53**, 1068-1089 (2024).
2. F. Strieth-Kalthoff, M. J. James, M. Teders, L. Pitzer, F. Glorius, Energy transfer catalysis mediated by visible light: principles, applications, directions. *Chem. Soc. Rev.* **47**, 7190-7202 (2018).

3. L. D. Elliott, S. Kayal, M. W. George, K. Booker-Milburn, Rational Design of Triplet Sensitizers for the Transfer of Excited State Photochemistry from UV to Visible. *J. Am. Chem. Soc.* **142**, 14947-14956 (2020).

4. R. Kleinmans *et al.*, Intermolecular [2π+2σ]-photocycloaddition enabled by triplet energy transfer. *Nature* **605**, 477-482 (2022).

5. S. O. Scholz, E. P. Farney, S. Kim, D. M. Bates, T. P. Yoon, Spin-Selective Generation of Triplet Nitrenes: Olefin Aziridination through Visible-Light Photosensitization of Azidoformates. *Angew. Chem. Int. Ed.* **55**, 2239-2242 (2016).

6. J. Majhi *et al.*, Metal-Free Photochemical Imino-Alkylation of Alkenes with Bifunctional Oxime Esters. *J. Am. Chem. Soc.* **144**, 15871-15878 (2022).

7. R. Kancherla *et al.*, Mechanistic insights into photochemical nickel-catalyzed cross-couplings enabled by energy transfer. *Nat. Commun.* **13**, 2737 (2022).

8. A. Dewanji, P. E. Krach, M. Rueping, The Dual Role of Benzophenone in Visible-Light/Nickel Photoredox-Catalyzed C-H Arylations: Hydrogen-Atom Transfer and Energy Transfer. *Angew. Chem. Int. Ed.* **58**, 3566-3570 (2019).

9. D. J. Keddie, A guide to the synthesis of block copolymers using reversible-addition fragmentation chain transfer (RAFT) polymerization. *Chem. Soc. Rev.* **43**, 496-505 (2014).

10. S. Perrier, 50th Anniversary Perspective: RAFT Polymerization—A User Guide. *Macromolecules* **50**, 7433-7447 (2017).

11. M. Chen, M. Zhong, J. A. Johnson, Light-Controlled Radical Polymerization: Mechanisms, Methods, and Applications. *Chem. Rev.* **116**, 10167-10211 (2016).

12. G. M. Miyake, J. C. Theriot, Perylene as an Organic Photocatalyst for the Radical Polymerization of Functionalized Vinyl Monomers through Oxidative Quenching with Alkyl Bromides and Visible Light. *Macromolecules* **47**, 8255-8261 (2014).

13. J. C. Theriot *et al.*, Organocatalyzed atom transfer radical polymerization driven by visible light. *Science.* **352**, 1082-1086 (2016).

14. D. A. Corbin, G. M. Miyake, Photoinduced Organocatalyzed Atom Transfer Radical Polymerization (O-ATRP): Precision Polymer Synthesis Using Organic Photoredox Catalysis. *Chem. Rev.* **122**, 1830-1874 (2022).

15. N. J. Treat *et al.*, Metal-free atom transfer radical polymerization. *J. Am. Chem. Soc.* **136**, 16096-16101 (2014).

16. Q. Ma *et al.*, Metal-free atom transfer radical polymerization with ppm catalyst loading under sunlight. *Nat. Commun.* **12**, 429 (2021).

17. J. Kreutzer, Dope new organocatalysts for ATRP. *Nat. Rev. Chem.* **5**, 73-73 (2021).

18. V. K. Singh *et al.*, Highly efficient organic photocatalysts discovered via a computer-aided-design strategy for visible-light-driven atom transfer radical polymerization. *Nat. Catal.* **1**, 794-804 (2018).

19. Z. Wu *et al.*, Selective Photoactivation of Trithiocarbonates Mediated by Metal Naphthalocyanines and Overcoming Activation Barriers Using Thermal Energy. *J. Am. Chem. Soc.* **144**, 995-1005 (2022).

20. J. Xu, S. Shanmugam, H. T. Duong, C. Boyer, Organo-photocatalysts for photoinduced electron transfer-reversible addition–fragmentation chain transfer (PET-RAFT) polymerization. *Polym. Chem.* **6**, 5615-5624 (2015).

21. Z. Wu, K. Jung, C. Boyer, Effective Utilization of NIR Wavelengths for Photo-Controlled Polymerization: Penetration Through Thick Barriers and Parallel Solar Syntheses. *Angew. Chem. Int. Ed.* **59**, 2013-2017 (2020).

22. X. Li, C. He, K. Matyjaszewski, X. Pan, ATRP of MIDA Boronate-Containing Monomers as a Tool for Synthesizing Linear Phenolic and Functionalized Polymers. *ACS Macro Lett.* **10**, 1327-1332 (2021).

23. J. Wang *et al.*, Photoinduced Metal-Free Atom Transfer Radical Polymerization of Biomass-Based Monomers. *Macromolecules* **49**, 7709-7717 (2016).

24. C. Zhou, Z. Zhang, W. Li, M. Chen, Organocatalyzed Photo-Controlled Synthesis of Ultrahigh-Molecular-Weight Fluorinated Alternating Copolymers. *Angew. Chem. Int. Ed.* **63**, e202314483 (2024).

25. S. Han *et al.*, Designing F/P Hybrid Polymer as Ultrastable Cationic Shielding Interphase for High-Performance Lithium Metal Batteries. *Angew. Chem. Int. Ed.* **62**, e202308724 (2023).

26. Q. Quan, M. Ma, Z. Wang, Y. Gu, M. Chen, Visible-Light-Enabled Organocatalyzed Controlled Alternating Terpolymerization of Perfluorinated Vinyl Ethers. *Angew. Chem. Int. Ed.* **60**, 20443-20451 (2021).

27. C. Lv, C. He, X. Pan, Oxygen-Initiated and Regulated Controlled Radical Polymerization under Ambient Conditions. *Angew. Chem. Int. Ed.* **57**, 9430-9433 (2018).

28. A. E. Enciso, L. Fu, A. J. Russell, K. Matyjaszewski, A Breathing Atom-Transfer Radical Polymerization: Fully Oxygen-Tolerant Polymerization Inspired by Aerobic Respiration of Cells. *Angew. Chem. Int. Ed.* **57**, 933-936 (2018).

29. E. Liarou *et al.*, Copper-Mediated Polymerization without External Deoxygenation or Oxygen Scavengers. *Angew. Chem. Int. Ed.* **57**, 8998-9002 (2018).

30. C. Kutahya, C. Schmitz, V. Strehmel, Y. Yagci, B. Strehmel, Near-Infrared Sensitized Photoinduced Atom-Transfer Radical Polymerization (ATRP) with a Copper(II) Catalyst Concentration in the ppm Range. *Angew. Chem. Int. Ed.* **57**, 7898-7902 (2018).

31. C. Bian, Y.-N. Zhou, J.-K. Guo, Z.-H. Luo, Aqueous Metal-Free Atom Transfer Radical Polymerization: Experiments and Model-Based Approach for Mechanistic Understanding. *Macromolecules* **51**, 2367-2376 (2018).

32. S. Poplata, A. Troster, Y. Q. Zou, T. Bach, Recent Advances in the Synthesis of Cyclobutanes by Olefin [2 + 2] Photocycloaddition Reactions. *Chem. Rev.* **116**, 9748-9815 (2016).

33. J. B. Metternich, R. Gilmour, A Bio-Inspired, Catalytic E --> Z Isomerization of Activated Olefins. *J. Am. Chem. Soc.* **137**, 11254-11257 (2015).

34. J. B. Metternich, R. Gilmour, One Photocatalyst, n Activation Modes Strategy for Cascade Catalysis: Emulating Coumarin Biosynthesis with (-)-Riboflavin. *J. Am. Chem. Soc.* **138**, 1040-1045 (2016).

35. N. J. Turro, V. Ramamurthy, J. C. J. P. Scaiano, Photobiology, Modern Molecular Photochemistry of Organic Molecules. **88**, (2012).

36. M. E. Best, P. H. Kasai, Electron spin resonance study of radicals in photopolymerized di(meth)acrylate network. *Macromolecules* **22**, 2622-2627 (1989).

37. D. C. Doetschman, R. C. Mehlenbacher, D. Cywar, Stable Free Radicals Produced in Acrylate and Methacrylate Free Radical Polymerization: Comparative EPR Studies of Structure and the Effects of Cross-Linking. *Macromolecules* **29**, 1807-1816 (1996).

38. A. Kajiwara, A. K. Nanda, K. Matyjaszewski, Electron Spin Resonance Study of Monomeric, Dimeric, and Polymeric Acrylate Radicals Prepared Using the Atom Transfer Radical Polymerization TechniqueDirect Detection of Penultimate-Unit Effects. *Macromolecules* **37**, 1378-1385 (2004).

39. R. X. E. Willemse, A. M. van Herk, E. Panchenko, T. Junkers, M. Buback, PLP−ESR Monitoring of Midchain Radicals in n-Butyl Acrylate Polymerization. *Macromolecules* **38**, 5098-5103 (2005).

40. A. Kajiwara, Time-Resolved Electron Spin Resonance Spectroscopy of Radicals Formed During Free Radical Polymerizations of Alkyl Acrylates. *Macromol. Rapid Commun.* **30**, 1975-1980 (2009).

41. N. Awwad, A. T. Bui, E. O. Danilov, F. N. Castellano, Visible-Light-Initiated Free-Radical Polymerization by Homomolecular Triplet-Triplet Annihilation. *Chem* **6**, 3071-3085 (2020).

42. D. H. Volman, G. S. Hammond, K. Gollnick, Advances in Photochemistry, Volume 14. (1988).

43. J. Zhao, S. Ji, H. Guo, Triplet–triplet annihilation based upconversion: from triplet sensitizers and triplet acceptors to upconversion quantum yields. *RSC Adv.* **1**, 937-950 (2011).

44. J. Zhou, Q. Liu, W. Feng, Y. Sun, F. Li, Upconversion luminescent materials: advances and applications. *Chem. Rev.* **115**, 395-465 (2015).

45. A. K. Le *et al.*, Singlet Fission Involves an Interplay between Energetic Driving Force and Electronic Coupling in Perylenediimide Films. *J. Am. Chem. Soc.* **140**, 814-826 (2018).

46. L. Ma, Y. Liu, H. Tian, X. Ma, Switching Singlet Exciton to Triplet for Efficient Pure Organic Room-Temperature Phosphorescence by Rational Molecular Design. *JACS Au* **3**, 1835-1842 (2023).

47. L. Ma, S. Sun, B. Ding, X. Ma, H. Tian, Highly Efficient Room‐Temperature Phosphorescence Based on Single‐Benzene Structure Molecules and Photoactivated Luminescence with Afterglow. *Adv. Funct. Mater.* **31**, 2010659 (2021).

48. C. A. Long, D. R. Kearns, Radiationless decay of singlet molecular oxygen in solution. II. Temperature dependence and solvent effects. *J. Am. Chem. Soc.* **97**, 2018-2020 (1975).

Author contributions:
Conceptualization: Jian Liu, Liangwei Ma, Xin Jin, Siyu Sun, He Tian and Xiang Ma
Experiment: Jian Liu, Meng Liu, Jun Du and Yaxiong Wei
Investigation: Jian Liu, Liangwei Ma, Xin Jin and Siyu Sun
Funding acquisition: Xiang Ma
Supervision: He Tian and Xiang Ma
Writing – original draft: Jian Liu
Writing – review & editing: Jian Liu, Yaxiong wei, Xinsheng Xu, Liangwei Ma, Siyu Sun, He Tian and Xiang Ma

Competing interests: The authors declare no conflict of interest.

Supplementary Materials:
Materials and Methods
Supplementary Text
Figs. S1 to S46
Tables S1 to S11
Coordinates of Molecular Structures
References